# Semi-Active Vibration Control of Train Suspension Using Optimized PID Controller

Shaimaa A. Ali[1,2], H. Metered[1*], A. M. Bassuiny[1,3], and Abdel Ghany M. Abdel Ghany[1, 4]

[1] *Helwan University, Cairo, Egypt*
[2] *High Institute of Engineering, Culture and Science City, Cairo, Egypt*
[3] *Faculty of Engineering, Heliopolis University, Cairo, Egypt*
[4] *Higher Engineering Institute, Thebes Academy, Cairo, Egypt*
[*]E-mail: Hassan.Metered@m-eng.helwan.edu.eg

## Abstract

Magnetorheological (MR) dampers emerge as highly advantageous semi-active mechanisms for vibration control within engineering systems, offering superior reliability and cost-effectiveness compared to active actuators, thus underscoring their significance in practical implementation. This research delves into the analysis of ride comfort in rail vehicles employing semi-active suspension control, examining its impact on the vertical dynamics of the train. The study employs the Harmony Search (HS) algorithm to optimize the gains of a proportional integral derivative (PID) controller, leveraging the self-adaptive global best harmony search method (SGHS) for its efficacy in minimizing tuning time and achieving optimal objective function values. The efficacy of the proposed controller is assessed through simulation of a quarter-rail vehicle model featuring six degrees of freedom (6-DOF) using MATLAB/Simulink software. Analysis of the simulated results demonstrates that the optimized PID controller markedly enhances ride comfort when compared to both passive suspension systems and conventional PID control strategies.

## Keywords

Magnetorheological Dampers, Rail vehicle suspension, Self-Adaptive Global Best Harmony Search Algorithm, and PID.

# 1 INTRODUCTION

During the last few decades, meta-heuristic optimization techniques inspired by physics, biology, and other fields have successfully been used in many engineering applications. The major purpose of optimization techniques is to get the best solution of the objective function depending on the decision variables under some specific constraints [1]. Genetic algorithm (GA), particle swarm optimization (PSO) algorithm, and ant colony optimization (ACO) algorithm are examples of meta-heuristic optimization techniques based on biology. Simulated annealing (SA) algorithm inspired by physics [2]. The Harmony Search (HS) algorithm is used in this study to tune the controllers' gains, which was introduced first by Woo [3] to emulate the behavior of music players producing perfect harmony together.

Various researchers applied the HS algorithm in different fields, for example, engineering, medicine, energy scheduling, computer science, and industry [1], [4], [5]. The HS method has several advantages, such as simplicity, limited adjustability, ease of use, and the capacity to balance exploitation with exploration while searching, in addition to its ability to combine with other meta-heuristic algorithms [2]. The PID controller parameters of an airflow control of a wells-turbine-based Oscillating-Water Column (OWC) were optimized using the SGHS by [6]. The SGHS algorithm was compared and evaluated using the optimized PID controller against the basic harmony search, improved harmony search, and global best harmony search algorithms. As a result of that investigation, better system performance was achieved by the SGHS algorithm.

Magnetorheological (MR) dampers are semi-active devices used in seat, primary, or secondary suspension for different types of vehicles. Semi-active control algorithms are necessary to control MR dampers, and damping force is generated and adapted accordingly. Two controllers are needed; a system controller is applied to find the demand force under specific road conditions, and a damper controller is used to get the command voltage applied to the MR damper coil [7]. The primary suspension is a vital system that connects the bogie and the wheelset and can mitigate vibration levels due to soil deformation. Active and semi-active vertical actuators have been used in conjunction with suspension springs to reduce and control the vertical vibrations of the train bogie. Skyhook and linear quadratic gaussian (LQG) control strategies are applied and compared to control primary vertical suspension [8]. The primary suspension is mainly for guiding the vehicle, and the secondary suspension is intended to enhance the vehicle's ride quality [9]. The secondary suspension is located between the vehicle body and the bogie to reduce transmitted excitations that reach the vehicle body.

Rail vehicles are the backbone of an integrated system because of their capacity and speed; they are becoming one of the most important and popular public transportation worldwide. Lately, statistics have reported that, in the past decade, the number of train passengers has increased by about 40% [10] Many researchers are motivated to minimize the vertical vibration transmitted to train passengers from rail irregularities to improve passenger comfort. The high levels of vibration annoy passengers and significantly affect human health due to the many hours spent riding trains. Unwanted vibrations due to track irregularities are affecting ride comfort [11]. The passenger is exposed to vibration for long hours, which causes health problems for him, especially low back pain [12], [13]. Many engineering and medical researchers studied the vibration effects on the passenger body and its ability to perform different activities on the train board [14], [12], [15], [16], [17], [18], [19], [20]. Over the past decades, many studies have investigated the reduction of vertical vibrations in railway vehicles. Either optimizing the lumped parameters or focusing on the structural stiffness of the system could minimize vertical vehicle vibrations. Due to the limitations of conventional passive

damping devices, controlled active and semi-active suspension systems attracted numerous researchers to obtain a compromise solution for the conflicting requirements of suspension systems [21]. The active suspension is crucial in ensuring good ride quality and tremendous flexibility in the vehicle's dynamic response. In contrast to the other types, an active suspension consists of an actuator that can deliver a force that is actively controlled by a control algorithm that uses data from connected vehicle sensors [22]. The well-known PID controller has been applied to the active rail vehicle secondary suspension to improve suspension performance [23]. The vertical motions of the active railway vehicle body and passenger have been controlled using optimized PID and optimized scaling factors of fuzzy logic controllers using GA [24]. Model predictive control technology based on a mixed control approach has been utilized for active vibration control of a railway vehicle [9]. Since semi-active suspensions combine the advantages of both active and passive suspensions, they have attracted a lot of attention and provided the best compromise between cost and performance [25]. Many applications can use MR semi-active suspensions, and many studies have focused on the secondary suspension of a train. A lot of previous publications mainly focused on the primary suspension or the vertical movement of the secondary suspension [26], [27], [28], [29]and [30].

PID controllers are commonly utilized in the industrial field because of their simple structure, ease of implementation, and robust performance, but conventional PID controllers with fixed parameters can hardly adapt to varying operating points in a wide range [31]. Recently, a multiple fuzzy PID suspension control system based on road recognition (MFRR) was applied to tune PID parameters online for a 2-DOF quarter vehicle model [32]. The MFRR was compared with the passive suspension system and traditional fuzzy PID and had better dynamic performance according to changes in road conditions. A fuzzy-self-tuning PID (FST PID) controller was implemented to enhance an active seat suspension system's performance to improve the pregnant woman's comfort [31]. An active seat suspension system incorporating a pregnant woman's body model consisting of 13-DOF was suggested to test suspension performance with the former controllers. To confirm the effectiveness of the suggested controllers, the controller comprised the FST PID and classic PID optimized using a genetic algorithm was compared with passive suspension system under bump and random road excitations. The results show that the merger of the GA and the FST PID controller significantly improved the comfort of the pregnant woman and her fetus.

A fuzzy PI/PD controller optimized by GA was proposed by [33] for an active vehicle suspension system. The results of the simulation showed that combining the GA and fuzzy controller can provide substantially greater driving comfort for passengers. Hybrid fuzzy and fuzzy-PID (HFFPID) controllers for a semi-active suspension of a 3-DOF quarter-car were published [34]. Simulation results illustrated that the HFFPID controller performs better than conventional suspension systems at reducing car body acceleration, suspension working space, and seat acceleration response. The back propagation neural network method was used to get the optimum PID parameters for an active 2-DOF quarter car model, with superlative results gotten by Levenberg-Marquardt algorithm training with 10 neurons in the one hidden layer [35]. The design of a neural network-based PID controller for a 2-DOF active suspension system was presented by Dahunsi [36]. Dahunsi compared the results of the proposed controller with those of a PID controller and showed better performance in terms of rise times and overshoots. ANFIS and ANN were compared to minimize error rates and average execution times by [37] who concluded that the hybrid learning algorithm of ANFIS works just as well as the backward spread of the ANN learning algorithm. Utilizing active suspension systems improves ride quality and passenger safety. These trucks' active suspensions may be able to lessen the negative impacts of the increasing vehicle body mass. Since the design of active and semi-active

suspensions must carefully consider the passengers' health and safety, ride comfort should be the focus of investigation.

The main contribution of the current article is to give a more thorough description of the behavior of a PID controller that has been optimized by SGHS and discuss how it might be used in a semi-active suspension system for rail vehicles for the first time. The results of this study recommend the use of the presented optimization technique in railway suspension systems. The rest of the paper is organized as follows: A description of the suspension model and the dynamic equations of motion are presented in Section 2. Section 3 provides the full details of PID system controller, damper controller, and the tuning process of controllers' gains using SGHS. Section 4 represents the simulation results obtained for PID, and optimized PID controllers, MR passive-on, MR passive-off, compared with passive suspension and discussed under sinusoidal and random rail tracks. Section 5 presents performance comparisons to facilitate the evaluation and comparison between all suspension systems Finally, Section 6 summarizes the conclusions.

## 2 Quarter-Rail Vehicle Dynamic Model

Quarter-rail vehicle dynamic model, which includes 6-DOF as shown in Fig. (1). This quarter model is investigated because of its relative simplicity for analysis rather than the full model, which is more accurate, but the increase in modeling complexity makes parameter identification difficult. The model takes passenger body weight into account as a model parameter to consider ride comfort. The 5-DOF quarter-rail vehicle model has been validated in ref. [23] and has been examined by real rail irregularities that have been measured by the KRAB track geometry measurement system. The model contains the mass of the rail vehicle body $m_c$, the mass of the bogie $m_b$, the inertia moment of the bogie $J_b$ and $m_{w1}, m_{w2}$ which are the masses of wheel sets that are located under the bogie. $K_2$ is secondary suspension stiffness, and $C_2$ is damping coefficients. $K_{11}$, $K_{12}$ and $C_{11}$, $C_{12}$ are stiffness and damping coefficients of primary suspension. $k_{h1}$ and $k_{h2}$ are the wheel-rail linear spring stiffness. In this study, seat dynamics are added to the 5-DOF to investigate ride comfort, as done by [24]. The passenger and seat frame mass is $m_p$ , the passenger seat suspension stiffness and damping coefficient are $K_p$ and $C_p$. The system inputs are rail irregularities that cause the vertical vibrations of sprung and unsprung masses ($Z_1$ is first wheel input and $Z_2$ is second wheel input).

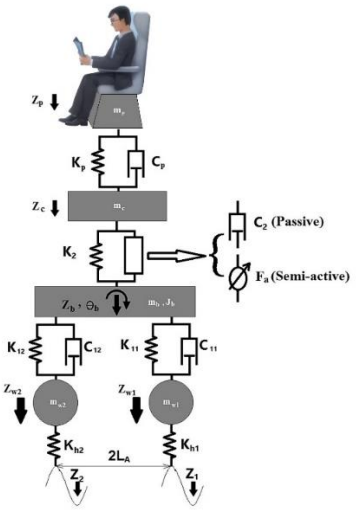


**Table 1 The 6-DOF rail vehicle model parameters [23], [24].**

| | | |
|---|---|---|
| $m_p$ = 80 kg | $K_p$=80000 N/m | $C_p$=40 Ns/m |
| $m_c$ = 8400 kg | $K_{11}$=12200000 N/m | $C_{11}$=4000 Ns/m |
| $m_b$ = 653.75 kg | $K_{12}$=12200000 N/m | $C_{12}$=4000 Ns/m |
| $m_{w1}$=453.25 kg | $K_2$=320000 N/m | $C_2$=20000 Ns/m |
| $m_{w2}$=453.25 kg | $K_{h1}$=1015549000 N/m | $L_A$=0.9 m |
| $J_b$ = 1121 kg.$m^2$ | $K_{h2}$=1015549000 N/m | |

Figure 1 Quarter Rail Vehicle Suspension Model, adapted from [23], [24].

$F_a$ is the control force which is generated by the MR damper which is placed between the rail vehicle body and the bogie. The half distance between the front and rear wheel sets is presented by $L_A$ and $V$ is the velocity of the rail vehicle. All the parameter values are given in Table (1), as introduced in [23], [24]. The six equations of motion of the quarter rail vehicle model with seat dynamics are derived using Newton's second law for semi-active MR suspension system as follows:

$$m_p\ddot{Z}_p - C_p(\dot{Z}_c - \dot{Z}_p) - K_p(Z_c - Z_p) = 0 \quad \ldots(1)$$

$$m_c\ddot{Z}_c + C_p(\dot{Z}_c - \dot{Z}_p) + K_p(Z_c - Z_p) - K_2(Z_b - Z_c) = F_a \quad \ldots(2)$$

$$m_b\ddot{Z}_b - C_{11}\left(\dot{Z}_{w1} - \dot{Z}_b - L_A\dot{\theta}_b\right) - C_{12}(\dot{Z}_{w2} - \dot{Z}_b + L_A\dot{\theta}_b) + K_2(Z_b - Z_c) - K_{11}(Z_{w1} - Z_b - L_A\theta_b) - K_{12}(Z_{w2} - Z_b + L_A\theta_b) = -F_a \quad \ldots(3)$$

$$J_b\ddot{\theta}_b - C_{11}L_A\left(\dot{Z}_{w1} - \dot{Z}_b - L_A\dot{\theta}_b\right) + C_{12}L_A(\dot{Z}_{w2} - \dot{Z}_b + L_A\dot{\theta}_b) - K_{11}L_A(Z_{w1} - Z_b - L_A\theta_b) + K_{12}L_A(Z_{w2} - Z_b + L_A\theta_b) = 0 \quad \ldots(4)$$

$$m_{w1}\ddot{Z}_{w1} + C_{11}\left(\dot{Z}_{w1} - \dot{Z}_b - L_A\dot{\theta}_b\right) + K_{11}(Z_{w1} - Z_b - L_A\theta_b) + K_{h1}Z_{w1} = K_{h1}Z_1 \quad \ldots(5)$$

$$m_{w2}\ddot{Z}_{w2} + C_{12}\left(\dot{Z}_{w2} - \dot{Z}_b + L_A\dot{\theta}_b\right) + K_{12}(Z_{w2} - Z_b + L_A\theta_b) + K_{h2}Z_{w2} = K_{h2}Z_2 \quad \ldots(6)$$

## 3 Rail Vehicle Secondary Suspension System Controller using MR dampers

A MR damper is an adjustable device that uses magnetorheological fluid as the carrier. Due to its low power consumption, quick reaction, simple control, and adjustable damping force, it is widely utilized in machinery, vehicles, and civil engineering applications [38]. The semi-active control algorithm for the suspension system model using an MR damper is shown in Fig. (2). It consists of two controllers; system and damper controllers. The system controller needs the dynamic outputs of the suspension to calculate the desired damper force $f_d$ according to the control algorithm. The damper controller computes the command voltage $v$ applied to the damper coil to generate the actual damper force $f_a$ that tracking the desired force $f_d$ . The following sub-sections provide the description of the system controller and the damper controller applied in this study.

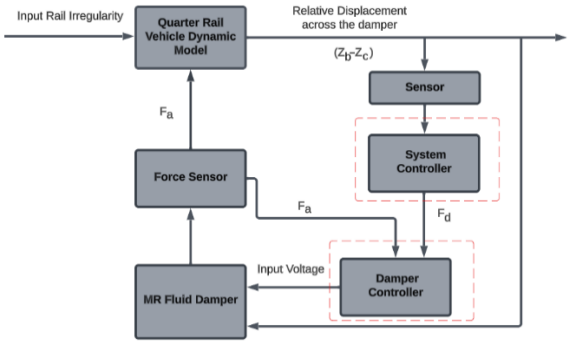


**Figure 2 The semi-active control algorithm for suspension system model.**

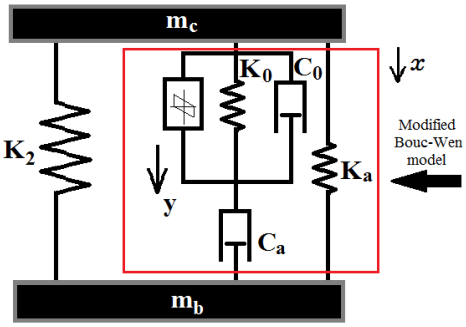


**Figure 3 Semi-active suspension incorporating Modified Bouc-Wen model.**

The modified Bouc-Wen model is the one that is most frequently used to depict the hysteretic effect of the MR damper. The Bouc-Wen model is named after Bouc, who first introduced the idea, and Wen, who generalized it [39]. Many researchers adopted Bouc-Wen models [40] due to their

extended ability to produce a variety of hysteretic behavior. Fig. (3) serves as an illustration for the mathematical model based on the modified Bouc-Wen model, which is fully discussed in [41].

Where;

$$F_a = C_a\,\dot{y} + k_a\,(x - x_o)\,,\; x = \; Z_b - Z_c \quad \ldots(7)$$

$$\dot{y} = \frac{1}{c_o + c_a}(\alpha Z + c_o\dot{x} + k_o(x - y)) \quad \ldots(8)$$

$$\alpha = \alpha_a + \alpha_b u \quad \ldots(9)$$

$$C_a = C_{aa} + C_{ab}u \quad \ldots(10)$$

$$C_o = C_{oa} + C_{ob}u \quad \ldots(11)$$

$$\dot{z} = -\gamma|\dot{x} - \dot{y}||z|^{n-1}z - \beta(\dot{x} - \dot{y})|z|^n + \delta(\dot{x} - \dot{y}) \quad \ldots(12)$$

$$\dot{u} = -\eta(u - v) \quad \ldots(13)$$

where, the internal displacement of the MR fluid damper is represented by y, $x_o$ is used to account for the effect of the accumulator. The output of a first-order filter is $u$ and $v$ is the command voltage sent to the current driver. The accumulator stiffness is $k_a$; the viscous damping observed at large, and low velocities are $c_o$and $c_a$, respectively. $k_o$ is present to control the stiffness at large velocities. The scaling value for this model is $\alpha$. The scale and shape of the hysteresis loop can be adjusted by $\gamma, \beta, \delta,$ and $n$. The model parameters are listed in Table *2* as used in previous published paper by [29].

**Table 2 Modified Bouc-Wen model parameters [29].**

| Parameter | value | Parameter | value |
|---|---|---|---|
| $C_{oa}$ | 2.1*10$^3$ Ns/m | $\alpha_a$ | 1.4*10$^4$ N/m |
| $C_{ob}$ | 3.5*10$^2$ Ns/Vm | $\alpha_b$ | 6.95*10$^4$ N/Vm |
| $k_o$ | 4.69*10$^3$ N/m | $\gamma$ | 3.63*10$^6$ 1/m$^2$ |
| $C_{aa}$ | 2.83*10$^4$ Ns/m | $\beta$ | 3.63*10$^6$ 1/m$^2$ |
| $C_{ab}$ | 2.95*10$^2$ Ns/Vm | $\delta$ | 301 |
| $k_a$ | 500 N/m | n | 2 |
| $x_o$ | 0.143 m | $\eta$ | 190 1/s |

The ride comfort for the rail vehicle passengers mainly depends on the control algorithm of the rail vehicle suspension system and the seat suspension system. The proposed control system is applied to the secondary suspension of the rail vehicle. The vibration control comparisons are held between three different suspension techniques: a) conventional passive oil damper, b) Passive-off (input voltage of MR damper=0V), c) Passive-on (input voltage of MR damper=12V), d) PID, and e) SGHS PID controlled secondary suspension systems.

### *3.1 PID Controller*

The PID is still the most popular controller that is widely used in the industry because of its structure simplicity, ease of implementation, and robust performance [31]. The PID controller force is given by Eq. 14 [42].

$$u(t) = k_p\, e(t) + k_i \int_0^t e(t)\, dt + k_d \frac{de(t)}{dt} \quad \ldots(14)$$

where, $k_p$, $k_i$, $k_d$ are proportional, integral, and differential gains respectively. Fig. (4) Indicates the block diagram of the PID controller optimized by using the SGHS technique with a multi-objective function, the set point is selected to be zero and the error is$Z_b - Z_c$.

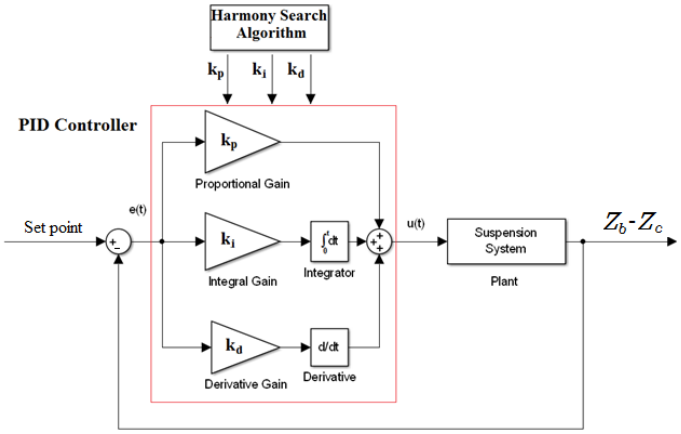


**Figure 4 Structure of Optimized PID controller.**

### *3.2 Self-Adaptive Global Best Harmony Search (SGHS) Algorithm*

The HS algorithm is used with the rail vehicle suspension system in this study to tune the PID parameters. HS is a phenomenon-imitating algorithm inspired by the improvisation process of music players. In the HS algorithm, each musician (decision variable) plays a note for finding the best harmony (global optimum) altogether.

The main parameters of the harmony algorithm are indicated as follows: harmony memory (HM), which represents the solution matrix, each row in the HM represents a solution vector. HM Size is the number of available solution vectors in the HM, number of rows in the solution matrix. Harmony Memory Consideration Rate (HMCR), which represents a number which determines the probability of selecting a solution from the existing HM solutions. Pitch Adjustment Rate (PAR) that represents a number which determines the probability of adjusting the selected solution within a certain range. Band Width (BW) that is the available range for adjusting the selected solution. The musical practices represent iterations limited to a maximum number of improvisations (NI). The jth variable's upper and lower bounds are denoted by UB(j) and LB(j), respectively, and r is a uniform random number between 0 and 1 [43]. Fig. (8) shows the flow chart of the SGHS algorithm. The HS tuning system parameters are demonstrated in Table 3.

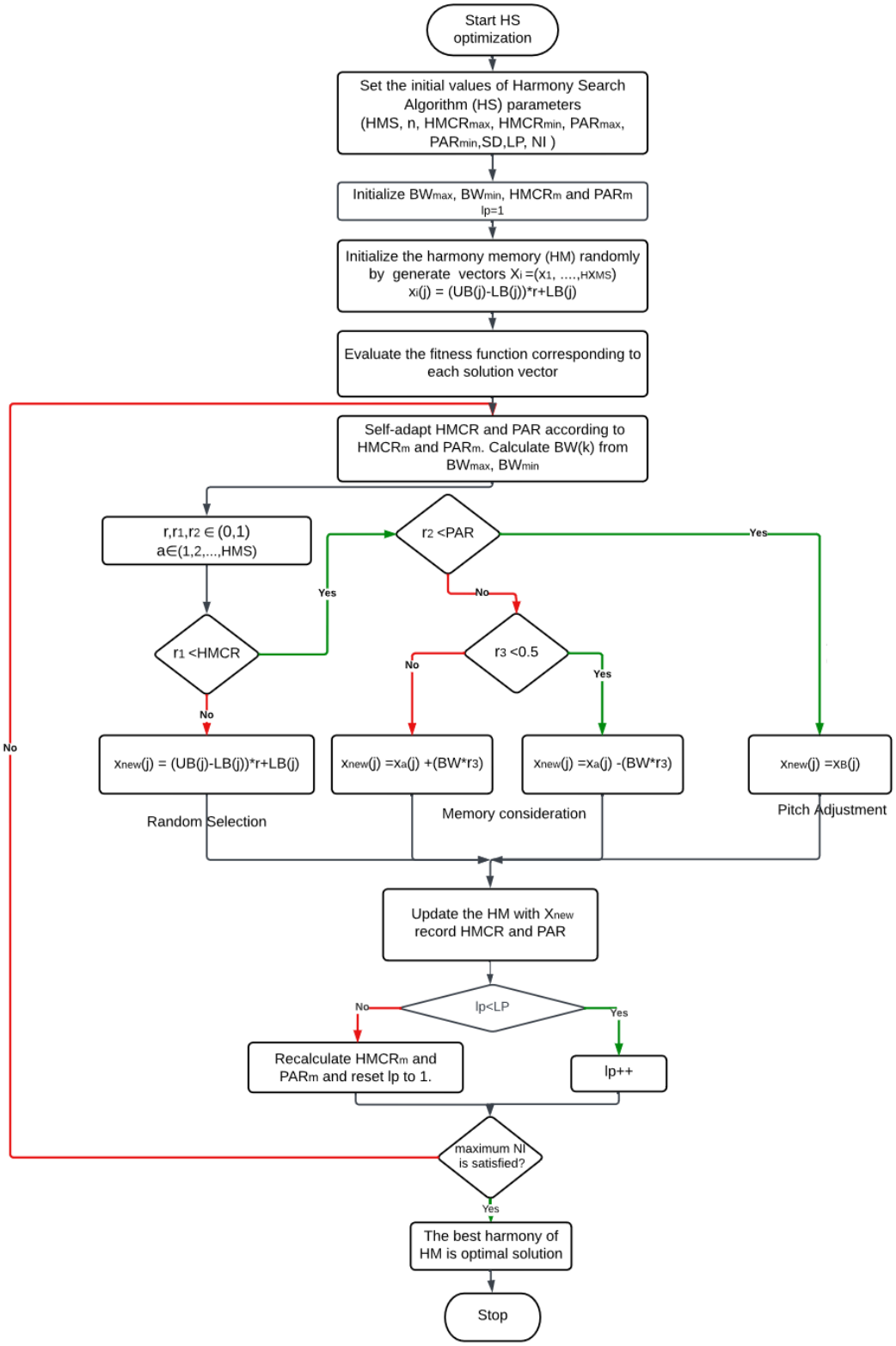


**Figure 5 the flow chart of the SGHS algorithm.**

. Three significant changes to the algorithm are presented by the SGHS:
(a) Self-adaptation of HMCR and PAR.
(b) Dynamic evolution of BW.
(c) New improvisation scheme.

**Table 3 Harmony search tuning system parameters.**

| HS parameters | Value |
|---|---|
| HMCR | 0.98 |
| HMS | 40 |
| PAR | 0.3 |
| BW | 0.01 |

The optimal design variables values can be obtained by the following multi-objectives function $f$, the aim is to minimize $f$. This function is derived by the combination of the peak-to-peak (PTP) values of the performance criteria, to improve the suspension performance on transient conditions, and the root mean square (RMS) values of the nominated criteria, to improve the suspension performance on realistic or random road condition [44].

$f$=$w_1$*PTP($\ddot{Z}_c$)+PTP($Z_c$) + $w_1 *$ PTP$\left(\ddot{Z}_p\right)$ + PTP$\left(Z_p\right)$ + $w_2 *$ PTP(STD)+ $w_1$*RMS($\ddot{Z}_c$)+ RMS($Z_c$) + $w_1 *$ RMS$\left(\ddot{Z}_p\right)$ + RMS$\left(Z_p\right)$ + $w_2 *$ RMS(STD) ... (15)

where, $\ddot{Z}_c$ is rail vehicle body acceleration, $Z_c$ is rail vehicle body displacement, $\ddot{Z}_p$is passenger seat vertical acceleration, $Z_p$ is passenger seat vertical displacement and STD is seat travel distance. The gains ($w_1$ and $w_2$) are chosen to magnify the small values of suspension outputs in Eq. (15).

By comparing the performance of our SGHS PID with the PID controller proposed in [23], we can show the effectiveness and efficiency of our optimization technique in this study. The parameters of PID and SGHS PID are shown in Table 4.

**Table 4 PID and SGHS PID parameters.**

| | PID | SGHS PID |
|---|---|---|
| $k_p$ | 6.27 * $10^5$ | 1094229.34 |
| $k_i$ | 100 | 2598523.67 |
| $k_d$ | 120 | 1452708.76 |

### *3.3 Damper controller*

The damper controller determines the DC voltage $v$ which commands the MR damper coil to produce a variable controllable actual damping force $F_a$ to track the desired damping force $F_d$ according to the following equation.

$$v = \frac{V_{max.}}{2N} \sum_{0 \le i \le N-1} \{sgn\{[F_d - (1 - ki)F_a]F_a\} + 1\} \quad \ldots(16)$$

where, sgn is the signum mathematical function, N is a positive integer and $0 \le i \le N-1$, k is a small constant, $V_{max.}$is the maximum input voltage to the current driver for the MR damper [29]. To determine the command voltage based on Eq. (16), N times of comparisons between the desired and the actual damping forces are required. For the ith comparison,

$$\begin{cases} \text{if } |F_d - (1-ki)F_a| > 0 & , v_i = \frac{V_{max.}}{2N} * 2 \\ \text{otherwise} & , v_i = \frac{V_{max.}}{2N} * 0 \end{cases} , \quad \ldots(17\text{-a})$$

$$v = \sum_{0 \le i \le N-1} v_i \quad \ldots(17\text{-b})$$

in this study, N=6, K=5*10$^{-4}$, and $V_{max.} = 12\ V$.

## 4 Results and discussion

To demonstrate the efficacy of the suggested semi-active suspension control systems, theoretical results are shown and discussed in this section. Five main criteria are selected to evaluate the effectiveness of the suggested system performance: rail vehicle body acceleration (RVBA), rail vehicle body displacement (RVBD), passenger seat acceleration (PSA), passenger seat vertical displacement (PSVD), and seat travel distance (STD). The results of the optimal controlled suspensions are compared to the passive suspension, as a base-line system, to determine the most suitable controller applied in this paper. Two types of road disturbances, sinusoidal and random track, are applied in this study to examine the effectiveness of proposed controllers.

### *4.1 Sinusoidal track profile*

The first type of disturbance is a sinusoidal track shown in Fig. (6), a 0.02 m amplitude, 3.125 Hz at the 90 km/h travelling speed as modelled in [23] for front and rear wheels. The time history of the rail suspension response under sinusoidal track excitation is shown in Figs. (7-11); RVBA, RVBD, PSA, PSVD, and STD, respectively. Passive represents the vehicle model without an MR damper and depends on a conventional damper. MR passive-off uses a zero-input voltage MR damper (When the control system fails, the semi-active suspension can still work under passive conditions.), while MR passive-on uses a maximum input voltage ($V_{max}$ = 12 volts) of the MR damper.

The latter figures show the comparison between the controlled semi-active, MR passive-off, MR passive-on and passive suspension systems. Based on the previous results, it's evidently seen that the controlled suspension systems dissipate the shock energy very well and improve suspension performance but the optimized PID using the SGHS algorithm gives a much better response.

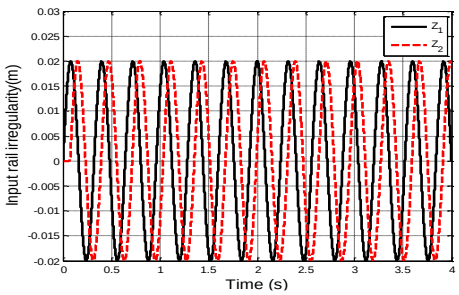


**Figure 6 Sinusoidal rail irregularity.**

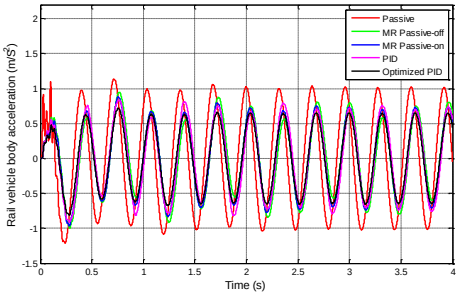


**Figure 7 Rail vehicle body acceleration.**

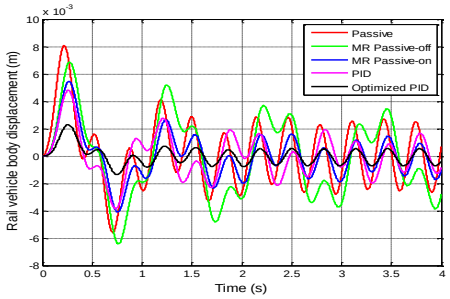


**Figure 8 Rail vehicle body displacement.**

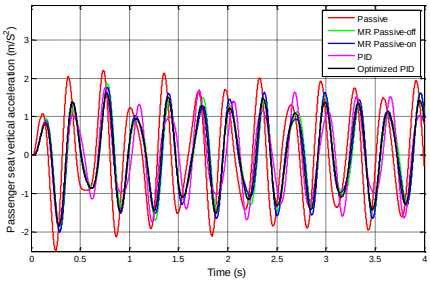


**Figure 9 Passenger seat vertical acceleration.**

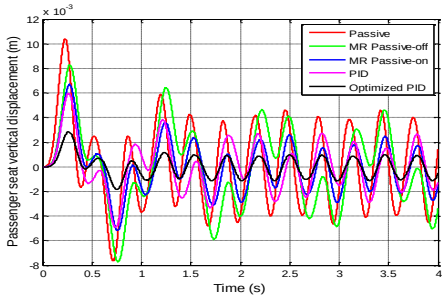


**Figure 10 Passenger seat vertical displacement.**

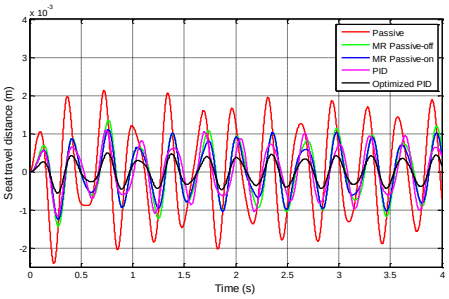


**Figure 11 Seat travel distance.**

### *4.2 Random track profile*

Random road disturbance is used as the second road profile applied in this paper to cause unwanted vehicle body vibrations. Muzaffer and Rahmi have measured the real random rail irregularities practically using a track geometry measurement system and simulated it as shown in Fig. (12) [23]. The RVBA, RVBD, PSA, PSVD, and STD responses under random road disturbance are shown in Figs. (13-17), respectively. The latter figures show the comparison between the controlled semi-active, MR passive-off, MR passive-on and passive suspension systems. . Like the results in sinusoidal road excitation, the controlled semi-active suspensions dissipate the energy due to random road excitation very well, reduce the vibration levels, and improve suspension performance but the optimized PID controller also gives a much better response.

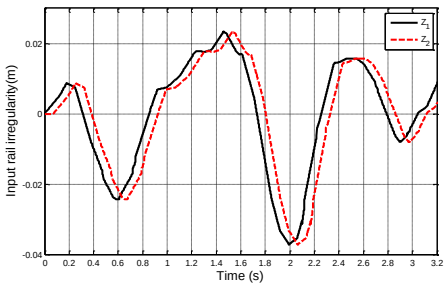


**Figure 12 Random rail irregularity.**

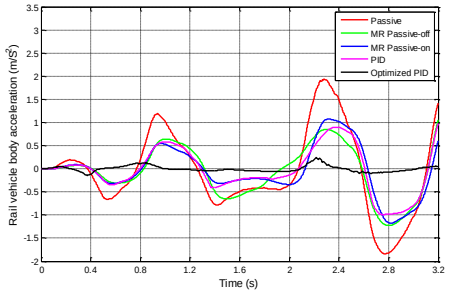


**Figure 13 Rail vehicle body acceleration ($m/s^2$).**

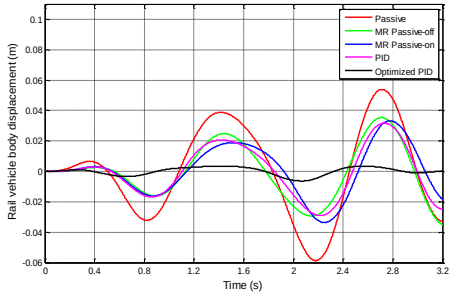


**Figure 14 Rail vehicle body displacement (m).**

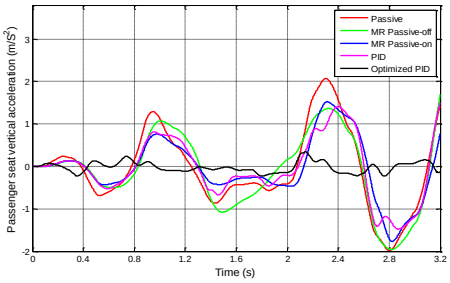


**Figure 15 Passenger seat vertical acceleration (m/s$^2$).**

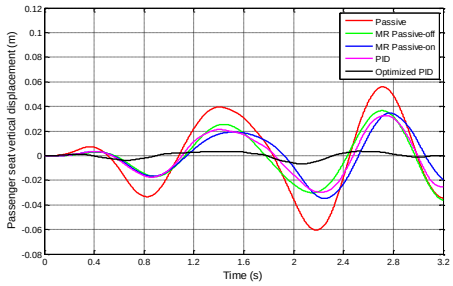


**Figure 16 Passenger seat vertical displacement.**

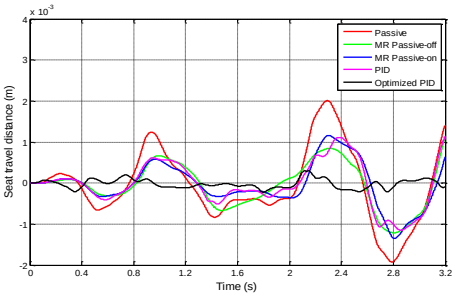


**Figure 17 Seat travel distance.**

### *4.3 Frequency domain results*

To examine the performance of the proposed controllers under frequency domain, a long random rail track is simulated and applied as a road input excitation which has the following specifications: 750 m length with a maximum urban transportation speed equal to 90 km/h [23], as shown in Fig. (18). Figures (19-23) demonstrate the modulus of the fast Fourier transform (FFT) of the RVBA, RVBD, PSA, PSVD, and STD, respectively, over the range 0.1–100 Hz under random rail track. The FFT is accurately smoothed by curve fitting. It's clearly seen that the response of the optimal PID controller is much lower than that of PID controller and the passive system also. According to the latter figures, the controlled semi-active suspensions dissipate the energy due to random road excitation very well and enhance the ride comfort, but the optimized PID controller can offer a superior performance.

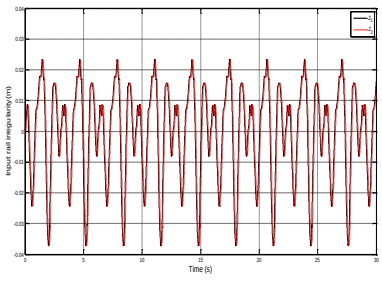


**Figure 18 Random rail irregularity for 30 seconds.**

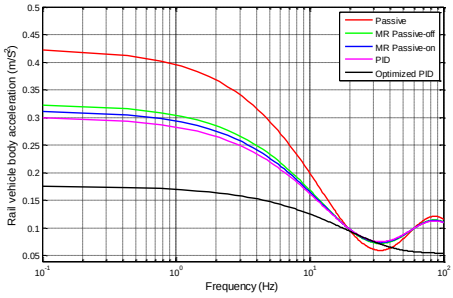


**Figure 19 Rail vehicle body acceleration in frequency domain.**

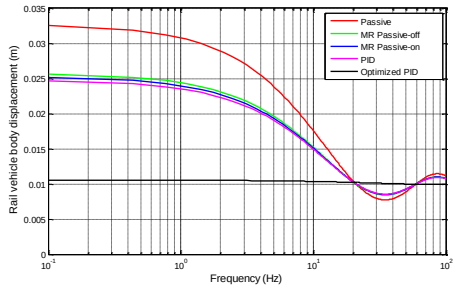


**Figure 20 Rail vehicle body displacement in frequency domain.**

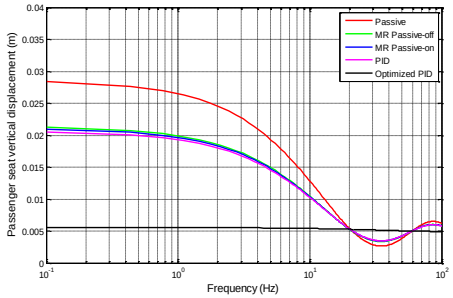


**Figure 21 Passenger seat vertical displacement in frequency domain.**

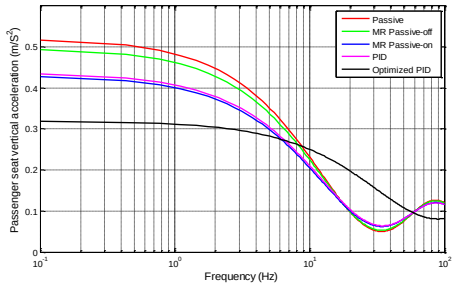


**Figure 22 Passenger seat vertical acceleration in frequency domain.**

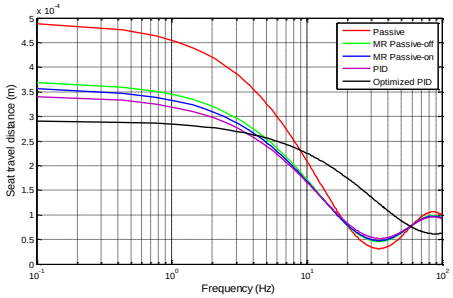


**Figure 23 Seat travel distance in frequency domain.**

### *4.4 The Dynamical Behavior of an MR damper*

The study introduces the dynamical behavior of an MR damper and compares the time history of the controlled damping force for PID and SGHS PID controllers Fig. (24), showing that the damper force has little changed despite improvements in SGHS PID response. Fig. (25) represents the corresponding command voltage.

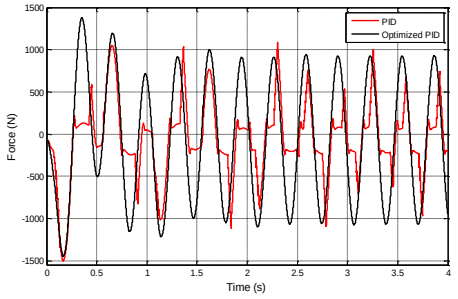


**Figure 24 Damping forces for MR damper controller**

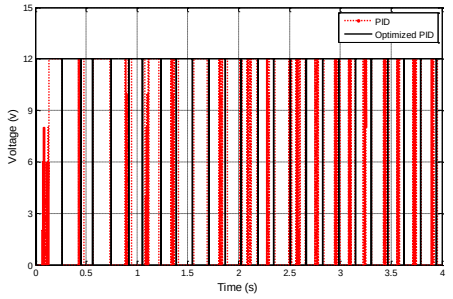


**Figure 25 corresponding command voltage of MR damper.**

## 5 Performance Comparisons

In this section, the percentage reduction index (PRI) (%) [45] is calculated to facilitate the evaluation and comparison between all suspension systems, PID, and optimized PID tuned by the

SGHS algorithm over the passive suspension. The five performance criteria stated above of semi-active suspensions are compared to the passive suspension in terms of PRI of peak-to-peak (PTP), based on Fig. (7-11), and root-mean-square (RMS), based on Fig. (13-17), using the following equation:

$$PRI = \frac{Passive-Semi-active}{Passive} X100 \ \ \% \qquad (18)$$

The peak-to-peak (PTP) values of the system response are listed in Table 5, which reflects that the semi-active controlled systems have lower peaks for all performance criteria demonstrating its success at improving the ride comfort over passive suspension. The root-mean-square (RMS) values of the system response are listed in Table 6, which shows that the semi-active controlled systems have the lower RMS for all performance criteria. Also, the calculated PRI of performance criteria for all controlled suspension over the passive system are calculated and listed in Tables 5 and 6. The numbers in Tables 5 and 6 show that the MR damper with both passive-off and passive-on control cases is capable of reducing the structural responses over the uncontrolled case, while the optimal PID can offer superior performance on sinusoidal and random road disturbances, demonstrating its efficiency at improving ride comfort.

**Table 5 PTP values and PRI under sinusoidal road irregularities.**

| | Passive | MR Passive-off | PRI % | MR Passive-on | PRI % | PID | PRI % | SGHS PID | PRI % |
|---|---|---|---|---|---|---|---|---|---|
| $\ddot{Z}_c$ (m/s$^2$) | 2.3514 | 1.8630 | 20.8% | 1.7406 | 26% | 1.6465 | 30% | 1.5318 | 34.9 % |
| $Z_c$ (m) | 0.0137 | 0.0133 | 2.8% | 0.0095 | 30.2 % | 0.0087 | 36.6 % | 0.0036 | 73.7 % |
| $Z_P$ (m) | 0.018 | 0.016 | 11% | 0.0119 | 34.2 % | 0.0109 | 39.7% | 0.0047 | 74 % |
| $\ddot{Z}_P$ (m/s$^2$) | 4.6819 | 3.8185 | 18.4% | 3.7578 | 19.7 % | 3.6079 | 22.9 % | 3.4647 | 26 % |
| STD (m) | 0.0045 | 0.0028 | 38.8% | 0.0024 | 47.9% | 0.0022 | 50.7% | 0.0011 | 76.6 % |

Table 6 RMS values and PRI under random rail irregularities

| | Passive | MR Passive-off | PRI % | MR Passive-on | PRI % | PID | PRI % | SGHS PID | PRI % |
|---|---|---|---|---|---|---|---|---|---|
| $\ddot{Z}_c$ (m/s$^2$) | 0.8573 | 0.5865 | 31.6% | 0.5576 | 35% | 0.5121 | 40.3% | 0.0780 | 90.9 % |
| $Z_c$ (m) | 0.0288 | 0.02 | 30.6% | 0.0188 | 34.9% | 0.0184 | 36.1% | 0.0023 | 92 % |
| $Z_P$ (m) | 0.0298 | 0.0206 | 30.8% | 0.0193 | 35.1% | 0.019 | 36.2% | 0.0024 | 91.9 % |
| $\ddot{Z}_P$ (m/s$^2$) | 1.0042 | 0.9401 | 6.4% | 0.7587 | 24.4% | 0.7428 | 26% | 0.1280 | 87.3 % |
| STD (m) | 9.8027* $10^{-4}$ | 5.8634* $10^{-4}$ | 40.1% | 5.8117*1 $0^{-4}$ | 40.7% | 5.7775* $10^{-4}$ | 41.1% | 1.1612* $10^{-4}$ | 88.2 % |

## 6 Conclusion

This study presented optimal PID, and PID controllers tuned using the self-Adaptive SGHS to enhance the performance of semi-active suspension of rail vehicles. A semi-active secondary rail suspension model incorporating an MR damper consisting of 6-DOF was derived and simulated using MATLAB/Simulink software. In order to judge the effectiveness of the applied controllers, system performance criteria were assessed in both time and frequency domains. The usage of the semi-active controlled MR damper in train suspensions offers a valuable improvement against the conventional passive system. It is shown that the MR damper with both passive-off and passive-on control cases is capable of reducing the structural responses over the uncontrolled case. Finally, the simulated results reflected that the optimal PID controller significantly improved ride comfort over the applied controllers.

## References

[1] F. Qin, A. M. Zain and K. Q. Zhou, "Harmony search algorithm and related variants:A systematic review," *Swarm and Evolutionary Computation,* vol. 74, 2022.

[2] P. Karthigeyan, M. S. Raja, R. Hariharan, S. Prakash, S. Delibabu and R. Gnanaselvam, "Comparison of harmony search algorithm, improved harmony search algorithm with biogeography based optimization algorithm for solving constrained economic load dispatch problems," *Procedia Technology,* vol. 21, p. 611 – 618, 6-8 August 2015.

[3] Z. Woo Geem, J. Hoon Kim and G. Loganathan, "A new heuristic optimization algorithm: Harmony Search Simulation," *Simulation,* vol. 76, pp. 60-68, 2001.

[4] A. Askarzadeh and E. Rashedi, "Harmony search algorithm, Basic concepts and Engineering applications," USA, 2018.

[5] D. Manjarres, I. Landa-Torres, S. Gil-Lopez, J. Ser, M.N.Bilbao, S.Salcedo-Sanz and Z.W.Geem, "A survey on applications of the harmony search algorithm," *Engineering Applications of Artificial Intelligence,* vol. 26, no. 8, pp. 1818-1831, 2013.

[6] F. M'zoughi, I. Garrido, A. J. Garrido and M. De La Sen, "Self-Adaptive Global-Best Harmony Search Algorithm-based airflow control of a wells-turbine-based oscillating-water column," *applied sciences,* vol. 10, no. 13, pp. 1-21, 2020.

[7] J. d. J. L. Santos, R. M. Menendez and A. R. Ricardo, "Semi-active control of automotive suspension systems with MR dampers," *Mathematical Problems in Engineering,* vol. 2012, pp. 1-21, 2012.

[8] Y. Sugahara and T. Kojima, "Suppression of vertical vibration in railway vehicle carbodies through control of damping force in primary suspension: presentation of results from running tests with meter-gauge car on a secondary line," *Computers in Railways : Railway Engineering Design and Operation,* vol. 181, pp. 329-337, 2018.

[9] P. E. Orukpe, X. Zheng, I. Jaimoukha, A. C. Zolotas and R. M. Goodall, "Model predictive control based on mixedH2/H∞ control approach for active vibration control of railway vehicles," *Vehicle System Dynamics,* vol. 46, no. 1, pp. 151-160, 2008.

[10] P. F. Silva and J. Mendes, "Passengers Comfort Perception and Demands on Railway Vehicles: A Review," in *International Congress on Engineering — Engineering for Evolution, KnE Engineering,*, 2020.

[11] C. Colin and G. Michael J., "Effects of vertical vibration on passenger activities: writing and drinking," *Ergonomics*, vol. 34, no. 10, pp. 1313-1332, 1991.

[12] M. Zaki Nuawi, A. Rasdan Ismail, J. Mohd Nor and M. Mustafizur Rahman, "Comparative study of whole-body vibration exposure between train and car passengers: A case study in Malaysia," *International Journal of Automotive and Mechanical Engineering (IJAME),* vol. 4, pp. 490-503, 2011.

[13] A. R. Ismail, M. Z. Nuawi, H. C.W., K. N. F., J. Mohd Nor and N. Kamilah Makhtar, "Whole Body Vibration Exposure to Train Passenger," *American Journal of Applied Sciences,* vol. 7 , no. 3, pp. 352-359, 2010.

[14] X. He, J. Chen, D. Tang, S. Peng and e. al., "Using an Inerter.Based Suspension to Reduce Carbody Flexible Vibration and Improve Riding.Comfort," *SAE Int. J. Veh. Dyn., Stab., and NVH* , vol. 7, no. 2, pp. 137-151, 2023.

[15] P. Nassiri, A. Koohpaei, H. Zeraati and P. Jafari Shalkouhi, "Train passengers comfort with regard to whole-body vibration," *Journal of Low Frequency Noise, Vibration and Active Control,* vol. 30 , no. 2, p. 125– 136, 2010.

[16] M. S. Khan and J. Sundstrom, "Effects of vibration on sedentary activities in passenger trains," *Journal of Low Frequency Noise, Vibration and Active Control*, vol. 26, no. 1, pp. 43-55, 2005.

[17] D. Connolly, G. Kouroussis, O. Laghrouche, C. Ho and M. Forde, "Benchmarking railway vibrations – Track, vehicle, ground and building effects.," *Construction and Building Materials,* vol. 92, pp. 64-81, 1 September 2015.

[18] E. Johanning, S. Fischer, E. Christ, B. Göres and P. Landsbergis, "Whole-Body vibration exposure study in U.S. railroad locomotives—An ergonomic risk assessment," *AIHA Journal*, vol. 63, no. 4, pp. 439-446, 2002.

[19] A. Mohammadi, L. A. Jimenez and F. Nasiri, "A Multi-Criteria Assessment of the Passengers' Level of Comfort in Urban Railway Rolling Stock," *Sustainable Cities and Society,* vol. 53, 2020.

[20] Y. Peng, Z. Wu, C. Fan, J. Zhou, S. Yi, Y. Peng and K. Ga, "Assessment of passenger long-term vibration discomfort: a field study in high-speed train environments," *Ergonomics ,* vol. 65, no. 2, pp. 1-13, 2021.

[21] A. Orvnas, "Methods for Reducing Vertical Carbody Vibrations of a Rail Vehicle," KTH Engineering Sciences, Stockholm, Sweden, 2010.

[22] H. Anis and B. Y. Noureddine, "Heavy trucks with intelligent control of active suspension based on artificial neural networks," *Proceedings of the Institution of Mechanical Engineers, Part I: Journal of Systems and Control Engineering,* vol. 235, no. 6, p. 952–969, 2021.

[23] M. Metin and R. Guclu, "Rail Vehicle Vibrations Control Using Parameters Adaptive PID Controller," *Hindawi Publishing Corporation Mathematical Problems in Engineering,* vol. 2014, pp. 1-10, 2014.

[24] M. Metin and R. Guclu, "Active vibration control with comparative algorithms of half rail vehicle model under various track," *Journal of Vibration and Control,* vol. 17, no. 10, pp. 1525-1539, 2011.

[25] F. Codecà, S. Savaresi, C. Spelta, M. Montiglio and M. Ieluzzi, "Semiactive Control of a Secondary Train Suspension.," Zurich, Switzerland,, 04-07 September 2007.

[26] V. Atray and P. Roschke, "Design, fabrication, testing, and fuzzy modeling of a large magnetorheological damper for vibration control in a railcar.," in *IEEE/ASME Joint Rail Conference*, Chicago, IL, USA, 24 April 2003.

[27] E. Foo and R. M. Goodall, "Active suspension control of flexiblebodied railway vehicles using electro-hydraulic and electro-magnetic actuators," *Control Engineering Practice,* vol. 8, no. 5, pp. 507-518, 2000.

[28] R. M. Goodall and W. Kortüm, "Mechatronic developments for railway vehicles of the future," *Control Engineering Practice,* vol. 10, no. 8, pp. 887-898, 2002.

[29] W. H. Liao and D. H. Wang, "Semiactive vibration control of train suspension systems via magnetorheological dampers," *Journal of Intelligent Material Systems and Structures,* vol. 14, no. 3, pp. 161-172, 2003.

[30] A. Stribersky, H. .. Müller and B. Rath, "The development of an integrated suspension control technology for passenger trains," *Proceedings of the Institution of Mechanical Engineers, Part F: Journal of Rail and Rapid Transit,* vol. 212, no. 1, pp. 33-42, 1998.

[31] S. A. Ali, H. Metered, A. Bassiuny and A. Abdel-Ghany, "Vibration Control of an Active Seat Suspension System Integrated Pregnant Woman Body Model," in *SAE Technical Paper 2019-01-0172*, United States, 02 Apr 2019.

[32] X. Ding, R. Li, Y. Cheng, Q. Liu and J. Liu., "Design of and research into a multiple-fuzzy PID suspension control system based on road recognition," *Processes,* vol. 9, no. 12, pp. 1-20, 2021.

[33] Y. P. Kuo and T. Li, "GA-based fuzzy PI/PD controller for automotive active suspension system," *IEEE Transactions on Industrial Electronics,* vol. 46, no. 6, p. 1051–1056, 1999.

[34] A. O. Bashir, X. Rui and J. Zhang, "Ride Comfort Improvement of a Semi-active Vehicle Suspension Based on Hybrid Fuzzy and Fuzzy-PID Controller," *Studies in Informatics and Control,* vol. 28, no. 4, pp. 421-430, 2019.

[35] H. Heidari and M. Homaei, "Design a PID controller for suspension system by back propagation neural network," *Hindawi Publishing Corporation Journal of Engineering,* pp. 1-9, 2013.

[36] O. A. Dahunsi, J. Pedro and O. T. Nyandoro, "System identification and neural network based PID control of servo - hydraulic vehicle suspension system," *South African Institute of Electrical Engineers,* vol. 101, no. 3, pp. 93-105, 2010.

[37] V. Gaur, A. Soni, P. Bedi and S. Muttoo, " Comparative analysis of ANFIS and ANN for evaluating inter-agent dependency requirements," *International Journal of Computer Information Systems and Industrial Management Applications,* vol. 6, p. 23–34, 2014.

[38] Z. Boqiang, H. Zhao and X. Zhang, "Adaptive variable domain fuzzy PID control strategy based on road excitation for semi-active suspension using continuous damping control(CDC )shock absorber," *Journal of Vibration and Control,* pp. 1-16, 2023.

[39] İ. Şahin, T. Engin and S. Cesmeci, "Comparison of some existing parametric models for magnetorheological fluid dampers," *Smart Materials and Structures,* vol. 19, no. 3, 2010.

[40] N. Kwok, Q. N. ,. Ha, J. Li and B. Samali, "A novel hysteretic model for magnetorheological fluid dampers and parameter identification using particle swarm optimization," *Sensors and Actuators A: Physical,* vol. 132, no. 2, pp. 441-451, 2006.

[41] H. Metered and Z. Šika, "Vibration control of a seat suspension system using magnetorheological damper," Senigallia, Italy, 2014.

[42] S. Nazemi, Masih-Tehrani and M. Masoud and Mollajafari, "GA tuned H∞ roll acceleration controller based on series active variable geometry suspension on rough roads," *International Journal of Vehicle Performance,* vol. 8, no. 2-3, pp. 166-187, 2022.

[43] M. Shamseldin, M. Abdel Ghany and Y. and Hendawey, "Optimal nonlinear PID speed control based on harmony search for an electric vehicle," *Future Engineering Journal ,* vol. 2, no. 1, 2021.

[44] H. El-taweel, M. M. Abd elhafiz and H. Metered, "Optimal lumped parameters estimation of vehicle passive suspension system using genetic algorithm," *Journal of Advances in Vehicle Engineering,* vol. 5, no. 1, pp. 34-44, 2018.

[45] Lau, L. YK and WH, "Design and analysis of magnetorheological dampers for train suspension," *Proceedings of the Institution of Mechanical Engineers, Part F: Journal of Rail and Rapid Transit,* vol. 219, no. 4, p. 261–276, 2005.